

NMR crystallography: The effect of deuteration on high resolution ^{13}C solid state NMR spectra of a 7-TM protein

K. Varga ^a, L. Aslimovska ^a, I. Parrot ^{b,d}, M.-T. Dauvergne ^{b,c}, M. Haertlein ^b,
V.T. Forsyth ^{b,d}, A. Watts ^{a,*}

^a Department of Biochemistry, University of Oxford, Oxford, OX1 3QU, UK

^b ILL-EMBL Deuteration Laboratory, Institut Laue Langevin, 6 Rue Jules Horowitz, BP 156, F-38042 Grenoble Cedex 9, France

^c EMBL Grenoble Outstation, 6 Rue Jules Horowitz, BP 181, F-38042 Grenoble Cedex 9, France

^d EPSAM/ISTM, Keele University Staffordshire ST5 5BG, UK

Received 20 July 2007; received in revised form 24 September 2007; accepted 27 September 2007

Available online 4 October 2007

Abstract

The effect of deuteration on the ^{13}C linewidths of U- ^{13}C , ^{15}N 2D crystalline bacteriorhodopsin (bR) from *Halobacterium salinarium*, a 248-amino acid protein with seven-transmembrane (7TM) spanning regions, has been studied in purple membranes as a prelude to potential structural studies. Spectral doubling of resonances was observed for receptor expressed in ^2H medium (for both 50:50% $1\text{H}:2\text{H}$, and a more highly deuterated form) with the resonances being of similar intensities and separated by <0.3 ppm in the methyl spectral regions in which they were readily distinguished. Line-widths of the methyl side chains were not significantly altered when the protein was expressed in highly deuterated medium compared to growth in fully protonated medium (spectral line widths were about 0.5 ppm on average for receptor expressed both in the fully protonated and highly deuterated media from the $\text{C}\delta$, $\text{C}\gamma_1$, and $\text{C}\gamma_2$ Ile ^{13}C signals observed in the direct, 21–39 ppm, and indirect, 9–17 ppm, dimensions). The measured ^{13}C NMR line-widths observed for both protonated and deuterated form of the receptor are sufficiently narrow, indicating that this crystalline protein morphology is suitable for structural studies. ^1H decoupling comparison of the protonated and deuterated bR imply that deuteration may be advantageous for samples in which low power ^1H decoupling is required.

© 2007 Elsevier B.V. All rights reserved.

Keywords: MMR crystallography; Membrane protein structure; Bacteriorhodopsin

1. Introduction

Perdeuteration has been used routinely in solution NMR for ^{13}C , ^{15}N labeled protein assignment studies required for structural descriptions (reviewed in [1]). The incorporation of ^2H into non-exchangeable positions decreases the rate of ^{13}C and $^1\text{H}(\text{N})$ T_2 relaxation and therefore increases the sensitivity and

resolution in multidimensional NMR experiments. The suppression of proton–proton scalar couplings (J_{HH}) as a result of deuteration further improves linewidths. Perdeuteration at all non-exchangeable protons can, as a consequence of these phenomena, significantly increase the size of proteins and protein complexes for which solution NMR resonance assignments and structural studies are possible. Thus, perdeuteration is a vital tool for membrane protein solution NMR structural studies, as large size of detergent micellar–protein complexes and inherent poor spectral resolution (due to the lack of assorted secondary structural elements) often hinder these studies [2].

In solid state NMR, deuteration has been mainly used as a tool to study protein and lipid dynamics and interactions [3–8]. It has also been shown that similarly to solution NMR studies, ^1H (N) linewidths are improved in deuterated proteins [9–15]. To date, only a few studies are available on the effect of deuteration

Abbreviations: bR, bacteriorhodopsin; 7TM, 7-transmembrane; NMR, nuclear magnetic resonance; MAS, magic angle spinning; DGK, diacylglycerol kinase; CP, cross polarisation; TPPM, two-pulse phase-modulated; Crh, catabolite repression histidine-containing phosphocarrier protein; DARR, dipolar assisted rotational resonance; DSS, 2,2-dimethyl-2-silapentane-5-sulfonate; S/N, single-to-noise ratio; CT, contact time; HETCOR, heteronuclear correlation

* Corresponding author.

E-mail address: awatts@bioch.ox.ac.uk (A. Watts).

on ^{13}C and ^{15}N linewidths of soluble, microcrystalline proteins [15–17] and none have been reported for membrane proteins. Moreover, the findings of these studies are inconsistent with each other. High resolution ^{13}C spectrum was obtained for ubiquitin at 18.8 T (800 MHz) and 20 kHz MAS frequency, where the linewidths were found to be identical between the protonated and perdeuterated samples when protons were decoupled [16]. Conversely, ^1H decoupling alone was not sufficient to achieve high resolution ^{13}C spectra of the α -spectrin SH3 domain at 14.1 T (600 MHz) and 25 kHz MAS frequency, and ^2H decoupling notably improved ^{13}C linewidths [17]. For another protein, Crh, at 11.74 T (500 MHz) and at 10 kHz MAS frequency, perdeuteration had an adverse affect on ^{13}C linewidths relative to the protonated Crh, which could not be recovered with ^2H decoupling [15], which may have been the result of a slightly less ordered sample. Other studies reported that deuteration influenced protein folding and assembly [18] and changed the crystal packing properties [19]. Here, the effect of deuteration of U- ^{13}C , ^{15}N enriched bacteriorhodopsin of *Halobacterium salinarium*, a 248 amino acid protein of seven-transmembrane (7TM) spanning helices is examined. The ^{13}C linewidths of heavily deuterated 50% deuterated, and non-deuterated U- ^{13}C , ^{15}N labeled bacteriorhodopsin 2D crystals in purple membranes, the native environment for bR are compared.

Although solid state NMR offers the advantage of studying membrane proteins in their native membrane environment, the challenges of spectroscopy are significantly greater than for soluble proteins. This is reflected in the fact that few partial assignments of extensively ^{13}C , ^{15}N enriched integral membrane proteins are available to date [20–28]. Although it has been established that soluble proteins give highly resolved spectra when in microcrystalline form, optimal sample preparation is still an ill-described area for membrane proteins. The available studies suggest, however, that sample conditions with higher order yield better linewidths as shown for diacylglycerol kinase (DGK) [29] and OmpG 2D [30]. As a result, the study of 2D and 3D crystalline proteins by solid state NMR ('NMR crystallography') has become more popular in recent years. Bacteriorhodopsin naturally forms 2D crystals in the purple membranes, thus good linewidths are anticipated, and bR can potentially serve as a case study for other membrane proteins, many of which can, for example, be formed into 2D arrays for electron diffraction studies.

2. Materials and methods

2.1. Samples

2.1.1. Growth-labeling

Three labeling schemes were employed in order to study the effect of deuteration on the bacteriorhodopsin purple membrane spectra. All three samples were U- ^{13}C , ^{15}N enriched, but differed in the extent of deuteration. One sample was grown in highly protonated medium (HCN-bR), one was grown in fully deuterated medium (DCN-bR; 100% D_2O), and the third was grown in medium containing 50/50 mixture of hydrogenated and deuterated material (HDCN-bR; 50% D_2O). *H. salinarium* (strain S9) was inoculated into Celtone® medium (Spectra Stable Isotopes) with the appropriate isotopic enrichment: Celtone-CN, for HCN-bR and, Celtone-dCN (50% deuterated) for DCN-bR and HDCN-bR. Labeled media (pH 6.46) were prepared by dissolving 5 g of Celtone® base powder, 250 g of NaCl, 2 g of KCl, 20 g of MgSO_4 , 0.2 g of

CaCl_2 , 3 g of sodium citrate, 2 mg biotine, and 2 mg thiamine in 1 l (final volume) of H_2O (HCN-bR), D_2O (DCN-bR) or 50/50 $\text{H}_2\text{O}/\text{D}_2\text{O}$ (HDCN-bR). The growth media were also supplemented with trace metals of MnSO_4 (0.3 $\mu\text{g}/\text{l}$), $\text{FeCl}_2 \cdot 4\text{H}_2\text{O}$ (3.6 $\mu\text{g}/\text{l}$), $\text{ZnSO}_4 \cdot 7\text{H}_2\text{O}$ (0.44 $\mu\text{g}/\text{l}$), and $\text{CuSO}_4 \cdot 5\text{H}_2\text{O}$ (0.05 $\mu\text{g}/\text{l}$). After 5 days of incubation (110 rpm, 37 °C, under illumination), when the optical density (at 660 nm) peaked, the cells were harvested. The growth in labeled medium was optimized and the DCN-bR and HDCN-bR were produced in the ILL Deuteration Laboratory (<http://www.ill.fr/deuteration>) at the Partnership for Structural Biology in Grenoble, France.

The purple membranes were purified according to the method of Oesterhelt and Stoekenius [31]. Purified bR was quantified by measuring the absorbance (at 565 nm; $\epsilon = 54,000 \text{ M cm}^{-1}$). The yield of the purified bR in purple membranes was estimated to be 17.3 mg, 5.5 mg, and 3.8 mg per liter of growth medium for HCN-bR, DCN-bR, and HDCN-bR respectively. In each case, the purple membranes were purified in buffers prepared with H_2O , thus the exchangeable deuterons were replaced by ^1H . Samples containing purified purple membrane were washed in MilliQ water and resuspended in 20 mM sodium citrate buffer (pH 6.0) containing 0.01% sodium azide, and the membranes were pelleted by centrifugation at $\sim 10,000 \times g$ for 24–36 h. Approximately the same amount of protein was packed (24–27 mg) for each preparation into 3.2 mm thin wall Varian solid state NMR rotors. The samples were sealed with a thin rubber disc to prevent dehydration during the NMR experiments. Samples measured over a period of time (some months) after storage at -20 °C, showed no changes.

2.2. Solid state NMR spectroscopy

All NMR experiments were carried out using an 18.8 T Varian/Magnex (^1H frequency = 800 MHz) wide-bore solid state NMR spectrometer equipped with a 3.2 mm HCN Balun probe operating at 799.16500 MHz and 200.96813 MHz for ^1H and ^{13}C . The spinning frequency was set to 10.776 kHz, and the apparent probe temperature was regulated to be -10 °C, although the actual sample temperature was higher (approximately $+5$ °C) due to spinning and proton decoupling. All experimental conditions were matched as closely as possible for the three different samples for valid comparison.

One dimensional (1D) (Fig. 1) spectra were collected using proton decoupling (30 ms; 74 kHz) during acquisition, and 1024 transients were signal averaged with 4 s pulse delay. The spectral width was set to 100.00 kHz. ^1H - ^{13}C cross polarization (CP) was achieved with a 57 kHz ^1H and 39–55 kHz tangent ramped ^{13}C pulse for 0.8 ms for CN-bR, and 1.25 ms for DCN-bR and HDCN-bR. CP buildup curves in Fig. 3 were acquired by arraying the contact time from 100 μs to 3.5 ms in steps of 100 μs during a ^1H - ^{13}C CP pulse at 58 kHz and 47 kHz (no ramp) for ^1H and ^{13}C respectively. The FIDs were collected for 20.0 ms. All 1D spectra were processed by sinebell square (cosine shifted) apodization and zero filled to 16K points before Fourier transformation in Spinsight (Varian). Signal-to-noise (S/N) and integral measurements were also carried out with Spinsight.

Two dimensional (2D) ^{13}C - ^{13}C homonuclear correlation spectra of bR were collected using the DARR pulse sequence [32] for 28 h for each sample. The number of acquisitions was 32 for each FID with 3 s pulse delay. The CP transfer conditions were the same as in the 1D spectra described in the above. During the data acquisition periods of 20.5 ms and 11.9 ms in the direct and indirect dimensions respectively, 74 kHz two-pulse phase-modulated (TPPM) [33] decoupling was applied on the ^1H channel. The dwell was set to 10.0 μs and 11.6 μs in the direct and indirect dimensions respectively. Homonuclear ^{13}C mixing was facilitated with an $n=1$ rotary resonance condition on the protons for a 15-ms mixing time. The spectra were apodized by cosine shifted sinebell window function and zero filled to 4K points in both dimensions. The carbon dimension was referenced externally to DSS using the downfield ^{13}C adamantane methylene peak at 40.48 ppm [34]. All 2D data were processed with NMRPipe [35] and the analysis was carried out using Sparky version 3.1 [36].

3. Results and discussion

3.1. Resolution

Fig. 1 shows the 1D spectra acquired at -10 °C of the three bR samples of various deuteration levels. The fully protonated

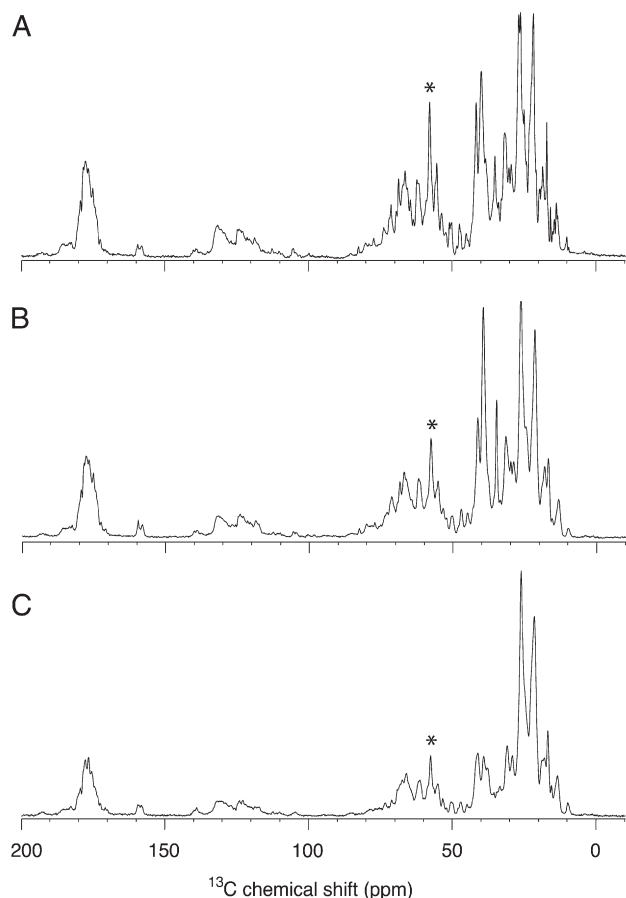


Fig. 1. 1D ^{13}C NMR spectra (800 MHz for ^1H) of CN-bR (A), HDCN-bR (B), and DCN-bR (C), with 24–27 mg of protein per sample fully hydrated in sodium citrate buffer (pH 6.0). The spectra were collected under very similar conditions, at -10°C and at a spinning frequency of 10.776 kHz. Each spectrum was signal averaged by 1K scans with 74.0 kHz ^1H decoupling for 30 ms. The $\text{C}\alpha$ 58 ppm resonance in CN-bR spectrum (57.7 ppm in DCN-bR) used for S/N measurements is identified (*).

(CN-bR) bR sample gave the highest apparent resolution in a 1D spectrum. The resolution of the highly deuterated DCN-bR 1D spectrum did not improve at different temperatures (arrayed from -20°C to $+20^\circ\text{C}$, data not shown). To investigate further the origin of the broadened lines of the 1D spectrum, 2D ^{13}C – ^{13}C DARR spectra were acquired, where the increased resolution of this method allows a comparison of some specific individual resonances. Comparison of the 2D ^{13}C – ^{13}C DARR spectra revealed that the individual peak resolution of the heavily deuterated (DCN-bR) sample is similar to the protonated bR (CN-bR), however marked peak doubling can be observed giving rise to the apparent reduced resolution observed in the 1D spectra of ^2H samples (Fig. 1). The alanine $\text{C}\beta$ – $\text{C}\alpha$ region of the 2D ^{13}C – ^{13}C DARR spectra of the three bR samples is shown in Fig. 2. The bacteriorhodopsin primary sequence contains 29 alanines, however at least five N- and C-terminal alanine crosspeaks are expected to be missing from the spectra due to time-averaged dipolar interactions, as shown by Saito and colleagues [37]. The alanines in the α -helices are likely to have similar chemical shifts due to their backbone positions. Due to spectral congestion, we were unable to count

the exact number of alanine crosspeaks in the ^{13}C – ^{13}C 2D spectra. However, at least 6 alanine resonances can be clearly resolved in the fully protonated bR (CN-bR) DARR spectrum (Fig. 2A). Although these 6 peaks can also be distinguished in the HDCN-bR spectrum in 2B, the resolution is greatly reduced due to peak multiplicity — the peaks are at least doubled or even tripled, as seen for peak 1 (Fig. 2B). Since the HDCN-bR sample was grown in 50/50 $^1\text{H}/^2\text{H}$ medium, this spectral multiplicity can be explained by the co-existence of ^1H – $^{13}\text{C}\alpha$ and ^2H – $\text{C}\alpha$ coupled to $^1\text{H}_3$ – $\text{C}\beta$, $^1\text{H}_2^2\text{H}$ – $\text{C}\beta$, $^1\text{H}^2\text{H}_2$ – $\text{C}\beta$, and $^2\text{H}_3$ – $\text{C}\beta$. In the spectrum from the highly deuterated bR (DCN-bR), apparent peak doubling is observed for the partially resolved peaks 3–6 (Fig. 2C). Resonances 1 and 2 in the DCN-bR spectra (Fig. 2C), which are resonances of the loop region as assigned previously by Saito and colleagues [38–40], are absent (compare with Fig. 2A and B). These amino acids are readily

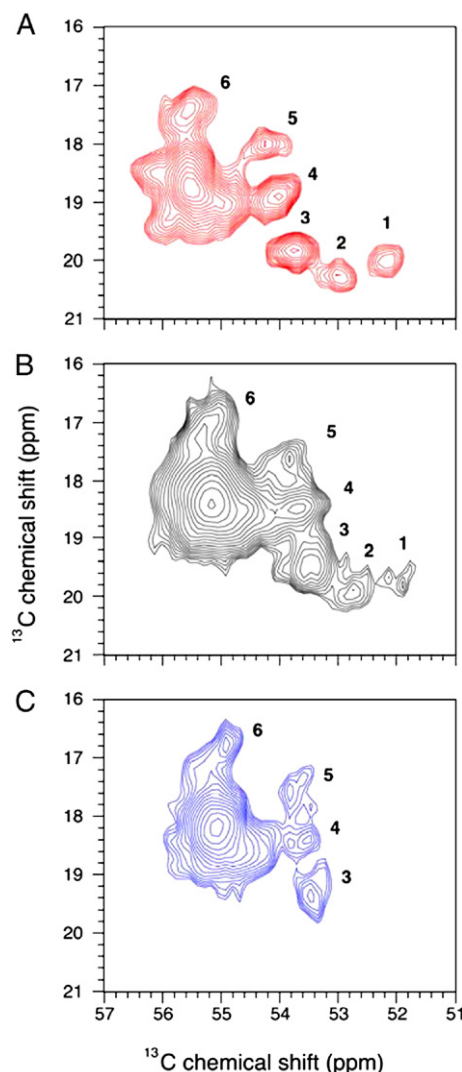


Fig. 2. Alanine $\text{C}\beta$ – $\text{C}\alpha$ region of CN-bR (A), HDCN-bR (B), and DCN-bR (C) from 2D ^{13}C – ^{13}C DARR spectra. The 6 resolved peaks of the CN-bR spectrum are numbered for easy reference and comparison between the spectra. All three spectra were acquired under identical conditions for all parameters except for the CT which was sample dependent. See Materials and methods for further experimental details and the text for discussion.

accessible to the ^1H 's in the buffer surrounding the loops which could serve as the source of cross-polarization. Thus resonances 1 and 2 are probably missing due to motion of the loops due to unfavorable protein dynamics. Of note is a ~ 0.3 – 0.5 ppm upfield shift of resonances in the HDCN-bR and DCN-bR spectra due to the deuterium isotope effect [41].

Another relatively well-resolved region of the 2D ^{13}C – ^{13}C DARR spectrum (not shown) was the isoleucine sidechain region (9–40 ppm). Peak doubling/multiplicity is also apparent in this region for the deuterated samples. The individual linewidths for the isoleucine $\text{C}\gamma_1$, $\text{C}\gamma_2$, and $\text{C}\delta$ crosspeaks were estimated to be 0.50–0.55 ppm (within measurement accuracy) for both DCN-bR and CN-bR samples when determined with the program NMRDraw [35]. Peak doubling was also seen in other regions of the DCN-bR 2D ^{13}C – ^{13}C DARR spectra, such as the $\text{C}\alpha$ – $\text{C}\beta$ region, although it is more difficult to distinguish these peaks due to spectral crowding.

Although the origin of the observed peak doubling is currently ambiguous, there are several possible explanations which could describe the data. Peak doubling may be attributed to two, although very similar conformations of bR present in the native purple membranes, since the chemical shifts are very similar, within 0.2–0.3 ppm. The ratio of the two forms is estimated to be roughly equal based on the signal-to-noise (S/N) of isolated peaks. Since the preparation of the purple membranes was similar in all the preparations examined, the two forms may have been induced during the expression of the purple membrane in *H. salinarium* in deuterated media, but not in

protonated media. Deuteration may have decreased the homogeneity of the bR crystals by interfering with protein conformation or 2D crystal packing, which has been observed for other deuterated proteins [18,19]. Since the growth medium was prepared from 50% deuterated Celtone powder (Celtone-dCN, 50%) dissolved in 50% D_2O (HDCN-bR) or 100% D_2O (DCN-bR), residual protonation could be a source of the presence of multiple resonances, which does not however account for the observation that the resonances have approximately the same intensity. Another possibility is that residual ^{13}C – ^2H couplings, which were not decoupled by MAS, caused peak doubling. This explanation is in agreement with a previous study of deuterated SH3, where deuterium decoupling improved spectral resolution of 1D spectra [17]. Our current setup did not allow for the deuterium decoupling, however it will be addressed in subsequent studies.

3.2. CP efficiency

One of the potential disadvantages of studying perdeuterated samples is the low efficiency of Cross Polarization in CP MAS experiments. All bR samples were purified in buffers prepared with H_2O , thus all exchangeable deuterons were replaced by protons. It has been reported that amide sites buried in the trans-membrane α -helices of bR are resistant to deuterium/proton exchange [42,43], thus only the loops might be expected to exchange the deuterons to protons, which could further decrease CP efficiency. Considering the potential disadvantage of

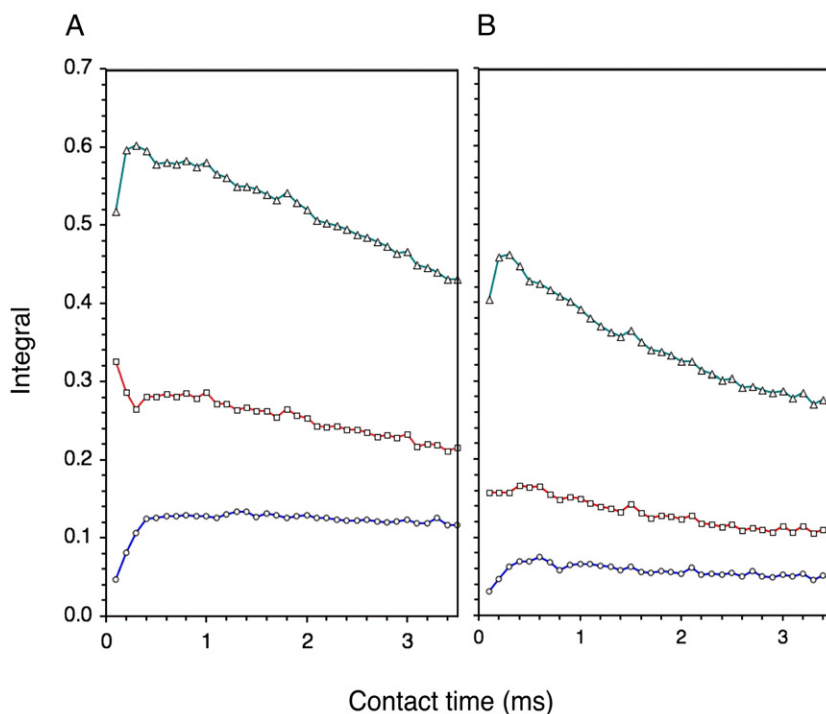


Fig. 3. CP buildup curves for the fully protonated CN-bR (A) and highly deuterated DCN-bR samples (B). The contact time was varied from 0.1 to 3.5 ms in steps of 0.1 ms and plotted vs. the integral of various regions of the spectra. The integrals of various regions of the 1D spectra were estimated by the program Spinsight to compare CP buildup: 164–189 ppm for CO (circles with blue line), 44–75 ppm for $\text{C}\alpha$ (squares connected with red line), and 9–44 ppm for the protein sidechain region (triangles and green line), which includes the lipid fatty acid chains. The integrals of DCN-bR sample were scaled to correct for any difference in sample amount ($\sim 11\%$).

deuteration, the CP efficiency of the highly deuterated DCN-bR was reasonably good compared to the protonated sample, as judged from the 1D spectra (Fig. 1).

In order to compare numerically the CP efficiency buildup rate of the highly deuterated DCN-bR and fully protonated CN-bR, CP buildup curves were determined (Fig. 3). The contact time during the ^1H – ^{13}C CP was varied and plotted against the integral of the spectral intensity of CO, $\text{C}\alpha$, and sidechain regions. It is difficult to make an accurate comparison of CP build-up behavior, however, since the setup of the CP can have a significant effect on the outcome. The comparison is further complicated by the presence of the lipid signals in the sidechain region, since the lipid fatty acid chain of the purple membranes are also uniformly isotopically enriched and overlap with sidechain region chemical shifts, as assigned by Tuzi et al. [44]. Here, no ramp was used during CP, and the contact time (CT) was arrayed. The same matching condition was used for both the protonated and deuterated samples ($5.4 \times \omega_{\text{R}}$ and $4.4 \times \omega_{\text{R}}$ for ^1H and ^{13}C , Fig. 3A and B respectively) and optimized on the sample for the best match. Although the match conditions were similar for the different regions, they were not the same; the match condition chosen was between the $\text{C}\alpha$ and CO signal. The CP buildup curves (Fig. 3) show that the CP buildup was only a little slower for the DCN-bR (Fig. 3B) sample relative to the CN-bR (Fig. 3A). The CP buildup is very fast for the $\text{C}\alpha$ spectral region of the protonated sample (0.1 ms), and for the DCN-bR where the buildup levels off after 0.4 ms contact time. CO buildup mostly levels off at 0.4 and 0.6 ms for the CN-bR (Fig. 3A) and the DCN-bR (Fig. 3B) samples respectively, although there is a small increase of integral at longer CT (>0.6 ms). The sidechains reach their maximum intensity at 0.3 ms for both samples. The curves were not corrected for relaxation. The above results imply that the more heavily deuterated proteins do not require significantly longer CT during CP when some protons are present.

For an estimation of the CP efficiency in the membrane samples, the largest integral from the CT buildup curve was taken. This comparison showed that the CP transfer efficiency of the DCN-bR relative to the CN-bR sample was 56%, 51%, and 77% for the CO, $\text{C}\alpha$, and the sidechain regions respectively. The sidechain CP efficiency here was consistently much stronger (77%) than observed for the ubiquitin example (40%) [16] even though the ubiquitin sample had protonated methyl groups, but as noted in the above, this region includes the resonances of the lipids from the purple membrane and therefore cannot be compared directly to ubiquitin, a soluble microcrystalline protein sample without lipids. Based on the observation from 2D ^{13}C – ^{13}C DARR spectra (for example, Fig. 2), most resonances present in the protonated spectrum are also observed in both deuterated bR (DCN-bR and HDCN-bR) 2D ^{13}C – ^{13}C DARR spectra under our experimental conditions (15 ms DARR mixing time). Although the observed resonances have a lower spectral intensity for DCN-bR, this is at least partly due to the reduced S/N from the ^1H – ^{13}C CP. These observations imply that sufficient amount of protons were present in the sample for both for ^1H – ^{13}C CP and DARR mixing even in a membrane protein which was produced in a highly deuterated, crystalline membrane environment.

In order to estimate which protons were involved in magnetization transfer to the carbons, 2D ^1H – ^{13}C heteronuclear correlation (HETCOR) spectra were acquired with various contact times (data not shown). The spectra revealed that at short contact time (0.1 ms) the CO receive the magnetization from the amide backbone H(N) which exchanged. The H(N) also transfer some magnetization to the $\text{C}\alpha$ carbons. However, strong $^{13}\text{C}\alpha$ – $^1\text{H}\alpha$ and sidechain ^{13}C –sidechain ^1H crosspeaks at 0.1 ms contact time confirm directly bonded protons to ^{13}C due to the partial protonation of the growth medium.

The effect of ^1H decoupling on the fully protonated CN-bR and highly deuterated DCN-bR samples was also investigated. Proton decoupling had less of an effect on the DCN-bR sample than on CN-bR sample as judged from 1D spectra where decoupling (continuous wave) was arrayed. For instance, the intensity of the $\text{C}\alpha$ resonance group at 58.0 ppm for CN-bR (at 57.7 ppm for DCN-bR) was measured in the 1D spectra (highlighted with asterisk in Fig. 1). When the decoupling decreased from 74.0 kHz to 43.0 kHz, for the DCN-bR the intensity decreased to only $\sim 86\%$ of the original value, while the intensity of the protonated CN-bR dropped to about $\sim 71\%$. Thus, high level of deuteration may be advantageous for samples for which the application of lower decoupling levels may be imperative for sample stability.

4. Conclusions

From these initial ^{13}C solid state NMR crystallography studies, it has been demonstrated here that U- ^{13}C , ^{15}N enriched bacteriorhodopsin yields high resolution spectra, where the line widths of ^{13}C spectra (0.5–0.6 ppm) are sufficient for further structural analyses using multidimensional approaches. The origin of peak doubling of the highly deuterated sample remains to be determined by future studies, but it is likely due to the high degree of sensitivity of NMR to sample heterogeneity caused by differential hydrophobic interactions between proteins, as shown for other systems [18,19]. It is unclear at the moment whether residual ^{13}C – ^2H couplings or differential isotropic shift due to the presence of proton could have contributed to the peak doubling. It has been found that deuteration may have benefits for samples in which low decoupling powers are needed and are little affected by covalent deuteration, except in the known isotope effect on chemical shifts. As a result of the sensitivity of chemical shifts to local differences in electronic field effects, sample homogeneity can be readily detected. Importantly, structural studies are potentially possible for membrane-embedded receptors although spectral crowding may need to be relieved by selective labeling [43].

Acknowledgements

We acknowledge financial support from EPSRC (under grants GR/R99393/01 and EP/C015452/1), Bionanotechnology IRC, Magnex Scientific and Varian Inc., and the advice from the staff of the ILL-EMBL Deuteration Laboratory. This work has benefited from the activities of the DLAB & JRA7 consortia funded by the EU under contracts HPRI-2001-50065 and RII3-CT-2003-505925.

References

- [1] K.H. Gardner, L.E. Kay, The use of H-2, C-13, N-15 multidimensional NMR to study the structure and dynamics of proteins, *Annu. Rev. Biophys. Biomol. Struct.* 27 (1998) 357–406 (I).
- [2] C.R. Sanders, F. Sonnichsen, Solution NMR of membrane proteins: practice and challenges, *Magn. Reson. Chem.* 44 (2006) S24–S40 (I).
- [3] M. Hologne, V. Chevelkov, B. Reif, Deuterated peptides and proteins in MAS solid-state NMR, *Prog. Nucl. Magn. Reson. Spectrosc.* 48 (2006) 211–232 (I).
- [4] A. Watts, in: G. Ceve (Ed.), *Phospholipids Handbook*, Marcel Dekker, New York, 1993, pp. 687–740.
- [5] P.T.F. Williamson, J.A. Watts, G.H. Addona, K.W. Miller, A. Watts, Dynamics and orientation of N+(CD3)3-bromoacetylcholine bound to its binding site on the nicotinic acetylcholine receptor, *Proc. Natl. Acad. Sci. U. S. A.* 98 (2001) 2346–2351 (I).
- [6] J.A. Watts, A. Watts, D.A. Middleton, A model of reversible inhibitors in gastric H⁺/K⁺-ATPase binding site determined by rotational echo double resonance NMR, *J. Biol. Chem.* 276 (2001) 43197–43204 (I).
- [7] D.A. Middleton, S. Rankin, M. Esmann, A. Watts, Structural insights into the binding of cardiac glycosides to the digitalis receptor revealed by solid-state NMR, *Proc. Natl. Acad. Sci. U. S. A.*, 97, 2000, pp. 13602–13607, (I).
- [8] S.L. Grage, A. Watts, Applications of REDOR for distance measurements in biological solids, *Annu. Rep. NMR* 60 (2007) 192–228 (I).
- [9] B. Reif, C.P. Jaronec, C.M. Rienstra, M. Hohwy, R.G. Griffin, H-1-H-1 MAS correlation spectroscopy and distance measurements in a deuterated peptide, *J. Magn. Reson.* 151 (2001) 320–327 (I).
- [10] E.K. Paulson, C.R. Morcombe, V. Gaponenko, B. Dancheck, R.A. Byrd, K.W. Zilm, Sensitive high resolution inverse detection NMR spectroscopy of proteins in the solid state, *J. Am. Chem. Soc.* 125 (2003) 15831–15836 (I).
- [11] V. Chevelkov, B.J. van Rossum, F. Castellani, K. Rehbein, A. Diehl, M. Hohwy, S. Steuernagel, F. Engelke, H. Oschkinat, B. Reif, H-1 detection in MAS solid-state NMR Spectroscopy of biomacromolecules employing pulsed field gradients for residual solvent suppression, *J. Am. Chem. Soc.* 125 (2003) 7788–7789 (I).
- [12] V. Chevelkov, K. Rehbein, A. Diehl, B. Reif, Ultrahigh resolution in proton solid-state NMR spectroscopy at high levels of deuteration, *Angew. Chem. Int. Ed.* 45 (2006) 3878–3881 (I).
- [13] C.R. Morcombe, E.K. Paulson, V. Gaponenko, R.A. Byrd, K.W. Zilm, H-1-N-15 correlation spectroscopy of nanocrystalline proteins, *J. Biomol. NMR* 31 (2005) 217–230 (I).
- [14] D.H. Zhou, D.T. Graesser, W.T. Franks, C.M. Rienstra, Sensitivity and resolution in proton solid-state NMR at intermediate deuteration levels: quantitative linewidth characterization and application to correlation spectroscopy, *J. Magn. Reson.* 178 (2006) 297–307 (I).
- [15] A. Bockmann, M. Juy, E. Bettler, L. Emsley, A. Galinier, F. Penin, A. Lesage, Water–protein hydrogen exchange in the micro-crystalline protein Crh as observed by solid state NMR, *J. Biomol. NMR* 32 (2005) 195–207 (I).
- [16] C.R. Morcombe, V. Gaponenko, R.A. Byrd, K.W. Zilm, C-13 CPMAS spectroscopy of deuterated proteins: CP dynamics, line shapes, and T-1 relaxation, *J. Am. Chem. Soc.* 127 (2005) 397–404 (I).
- [17] V. Agarwal, A. Diehl, N. Skrynnikov, B. Reif, High resolution H-1 detected H-1,C-13 correlation spectra in MAS solid-state NMR using deuterated proteins with selective H-1,H-2 isotopic labeling of methyl groups, *J. Am. Chem. Soc.* 128 (2006) 12620–12621 (I).
- [18] S. Yokogaki, K. Unno, N. Oku, S. Okada, Chaperonin-repairable subtle incompleteness of protein assembly induced by a substitution of hydrogen with deuterium — effect of groe on deuterated ribulose 1,5-bisphosphate carboxylase, *Plant Cell Physiol.* 36 (1995) 419–423 (I).
- [19] X. Liu, B.L. Hanson, P. Langan, R.E. Viola, The effect of deuteration on protein structure: a high-resolution comparison of hydrogenous and perdeuterated haloalkane dehalogenase, *Acta Crystallogr., D Biol. Crystallogr.* 63 (2007) 1000–1008 (I).
- [20] T.A. Egorova-Zachernyuk, J. Hollander, N. Fraser, P. Gast, A.J. Hoff, R. Cogdell, H.J.M. de Groot, M. Baldus, Heteronuclear 2D-correlations in a uniformly C-13, N-15 labeled membrane–protein complex at ultra-high magnetic fields, *J. Biomol. NMR* 19 (2001) 243–253 (I).
- [21] A.J. van Gammeren, F. Buda, F.B. Hulsbergen, S. Kiihne, J.G. Hollander, T.A. Egorova-Zachernyuk, N.J. Fraser, R.J. Cogdell, H.J.M. de Groot, Selective chemical shift assignment of B800 and B850 bacteriochlorophylls in uniformly [C-13,N-15]-labeled light-harvesting complexes by solid-state NMR spectroscopy at ultra-high magnetic field, *J. Am. Chem. Soc.* 127 (2005) 3213–3219 (I).
- [22] A.J. van Gammeren, F.B. Hulsbergen, J.G. Hollander, H.J.M. de Groot, Residual backbone and side-chain ¹³C and ¹⁵N resonance assignments of the intrinsic transmembrane light-harvesting 2 protein complex by solid-state Magic Angle Spinning NMR spectroscopy, *J. Biomol. NMR* 31 (2005) 279 (I).
- [23] A. Lange, K. Giller, S. Hornig, M.-F. Martin-Eauclaire, O. Pongs, S. Becker, M. Baldus, Toxin-induced conformational changes in a potassium channel revealed by solid-state NMR, *Nature* 440 (2006) 959 (I).
- [24] A. Lange, K. Giller, O. Pongs, S. Becker, M. Baldus, Two-dimensional solid-state NMR applied to a chimeric potassium channel, *J. Recept. Signal Transduct. Res.* 26 (2006) 379–393 (I).
- [25] K. Varga, L. Tian, A.E. McDermott, Solid State NMR Study and Assignments of the KcsA Potassium Ion Channel of *S. lividans*, (submitted for publication).
- [26] M. Etkorn, S. Martell, O.C. Andronesi, K. Seidel, M. Engelhard, M. Baldus, Secondary Structure, Dynamics, and Topology of a Seven-Helix Receptor in Native Membranes, Studied by Solid-State NMR Spectroscopy, *Angew. Chem. Int. Ed.* 9999 (2006) (NAI).
- [27] S. Jehle, M. Hiller, K. Rehbein, A. Diehl, H. Oschkinat, B.J. van Rossum, Spectral editing: selection of methyl groups in multidimensional solid-state magic-angle spinning NMR, *J. Biomol. NMR* 36 (2006) 169–177 (I).
- [28] M. Kobayashi, Y. Matsuki, I. Yumen, T. Fujiwara, H. Akutsu, Signal assignment and secondary structure analysis of a uniformly [¹³C, ¹⁵N]-labeled membrane protein, H⁺-ATP synthase subunit c, by magic-angle spinning solid-state NMR, *J. Biomol. NMR* 36 (2006) 279–293 (I).
- [29] M. Lorch, S. Fahem, C. Kaiser, I. Weber, A.J. Mason, J.U. Bowie, C. Glaubitz, How to prepare membrane proteins for solid-state NMR: a case study on the alpha-helical integral membrane protein diacylglycerol kinase from *E. coli*, *ChemBioChem* 9 (2005) 1693–1700 (I).
- [30] M. Hiller, L. Krabben, K.R. Vinothumar, F. Castellani, B.J. van Rossum, W. Kuhlbrandt, H. Oschkinat, Solid-state magic-angle spinning NMR of outer membrane protein G from *Escherichia coli*, *ChemBioChem* 6 (2005) 1679–1684 (I).
- [31] D. Oesterhelt, W. Stoekenius, Isolation of the cell membrane of *Halo-bacterium halobium* and its fractionation into red and purple membrane, *Methods Enzymol.* 31 (1974) 667–678 (I).
- [32] K. Takegoshi, S. Nakamura, T. Terao, C-13-H-1 dipolar-assisted rotational resonance in magic-angle spinning NMR, *Chem. Phys. Lett.* 344 (2001) 631–637 (I).
- [33] A.E. Bennett, C.M. Rienstra, M. Auger, K.V. Lakshmi, R.G. Griffin, Heteronuclear decoupling in rotating solids, *J. Chem. Phys.* 103 (1995) 6951–6958 (I).
- [34] C.R. Morcombe, K.W. Zilm, Chemical shift referencing in MAS solid state NMR, *J. Magn. Reson.* 162 (2003) 479–486 (I).
- [35] F. Delaglio, S. Grzesiek, G.W. Vuister, G. Zhu, J. Pfeifer, A. Bax, NMRpipe — a multidimensional spectral processing system based on unix pipes, *J. Biomol. NMR* 6 (1995) 277–293 (I).
- [36] D.T. Goddard, D.G. Kneller, in *University of California*, San Francisco.
- [37] S. Tuzi, A. Naito, H. Saito, ¹³C NMR study on conformation and dynamics of the transmembrane alpha-helices, loops, and C-terminus of [3-¹³C]Ala-labeled bacteriorhodopsin, *Biochemistry* 33 (1994) 15046–15052 (I).
- [38] H. Saito, Dynamic pictures of membrane proteins in two-dimensional crystal, lipid bilayer and detergent as revealed by site-directed solid-state NMR ¹³C NMR, *Chem. Phys. Lipids* 132 (2004) 101–112 (I).
- [39] H. Saito, G.A. Webb, *Annual Reports on NMR Spectroscopy*, Academic Press, 2006, pp. 99–175.
- [40] H. Saito, Y. Kawase, A. Kira, K. Yamamoto, M. Tanio, S. Yamaguchi, S. Tuzi, A. Naito, Surface and dynamic structures of Bacteriorhodopsin in a 2D crystal, a distorted or disrupted lattice, as revealed by site-directed solid-state ¹³C NMR, *Photochem. Photobiol.* 83 (2007) 253–262 (I).

- [41] D.G. Morris, M.A. Murray, Carbon-13 chemical shifts and substituent effects in 4-substituted camphors, N-nitrocamphorimines, and diazocamphors, *J. Chem. Soc., Perkin Trans 2* (1976) 1579–1584 (I).
- [42] T.N. Earnest, J. Herzfeld, K.J. Rothschild, Polarized Fourier transform infrared spectroscopy of bacteriorhodopsin, *Biophys. J.* 58 (1990) 1539–1546 (I).
- [43] A.J. Mason, S.L. Grage, C. Glaubitz, S.K. Strauss, A. Watts, Identifying anisotropic constraints in multiply labelled membrane proteins by ^{15}N MAS NMR, *Biophys. J.* 86 (2004) 1610–1617 (I).
- [44] S. Tuzi, A. Naito, H. Saito, A high-resolution solid-state ^{13}C -NMR study on $[1-^{13}\text{C}]\text{Ala}$ and $[3-^{13}\text{C}]\text{Ala}$ and $[1-^{13}\text{C}]\text{Leu}$ and Val-labelled bacteriorhodopsin. Conformation and dynamics of transmembrane helices, loops and termini, and hydration-induced conformational change, *Eur. J. Biochem.* 218 (1993) 837–844 (I).